Amorphous porous M_xTi mixed oxides as catalysts for the oxidative dehydrogenation of ethylbenzene

Wen Ying Li *, Christian Lettmann and Wilhelm F. Maier **

Max-Planck-Institut for Kohlenforschung, Kaiser-Wilhelm Platz 1, D-45470 Mülheim an der Ruhr, Germany
E-mail: maier@mpi-muelheim.mpg.de

Received 13 September 1999; accepted 2 August 2000

The properties of different metal-oxide-doped porous titanium oxides as catalysts for the oxidative dehydrogenation of ethylbenzene were investigated. Amorphous porous mixed oxides based on the amorphous titania matrix with selected metal ion centers as active sites have been prepared by an acid-catalyzed sol–gel method. The dehydrogenation of ethylbenzene was studied in a continuous gas phase flow reactor under different reaction temperatures at ambient pressure. Among the 23 catalysts studied the amorphous porous AM-Cr_5Ti mixed oxide is the most promising catalyst. At 350 °C a 75% selectivity to styrene at a 29% conversion of ethylbenzene was obtained. BET, HRTEM, XRD, GC, MS, TGA and optical microscopy were employed to characterize the fresh and used AM-Cr_5Ti catalyst.

Keywords: amorphous porous mixed oxides, catalyst, oxidative dehydrogenation, ethylbenzene, styrene

1. Introduction

In light of its attractive physical and chemical properties (thermal, mechanical and chemical resistance), titanium-oxide-based catalysts are increasingly used in heterogeneous catalysis, preferentially in selective oxidation reactions. Recent examples are the oxidative dehydrogenation of light alkanes [1,2] or the selective oxidation of toluene to benzoic acid over a V_2O_5/TiO_2 system [3,4]. However, there are only few reports where the titania-based catalyst is produced by a sol–gel procedure [5]. Large surface area TiO_2 can be prepared by the sol–gel process. Even microporous TiO_2 with a narrow pore size distribution has already been reported [6]. In a recent review the potential of the sol–gel method to tailor microporous or mesoporous structures in solids has been emphasized as one of the advantages relative to other catalyst preparation procedures [7]. Besides a report on unusual photocatalytic properties with visible light of Pt-doped amorphous porous TiO_2 [8], there is no information on the catalytic properties of titania-based catalysts produced by the sol–gel method. Even less is known about the effect of dopants (active sites) on the catalytic activity of such oxidation catalysts. The above mentioned reports utilize impregnated TiO_2 as catalysts. In the present study we present first results on the activity of porous TiO_2 containing 3–5 mol% of selected transition metal oxides as catalytically active centers. The oxidative dehydrogenation reaction of ethylbenzene to styrene in the gas phase was chosen as a model reaction. Oxidative dehydrogenation of ethylbenzene with synthetic air is a highly exothermic reaction,

$$C_6H_5\text{–}C_2H_5 + \tfrac{1}{2}O_2 \rightarrow C_6H_5\text{–}C_2H_3 + H_2O,$$
$$\Delta H^0_{298} = -124.7 \text{ kJ/mol},$$

which has the potential to be carried out at total conversion, if secondary reactions can be avoided.

Catalytic dehydrogenation of ethylbenzene is of importance for the manufacture of styrene, a comodity of still increasing demand. Styrene is presently produced by two processes, the dehydrogenation of ethylbenzene [9] and as a coupling product in the production of propylene oxide in related heterogeneously [10] and in homogeneously catalyzed reactions [11]. Main drawbacks of the dehydrogenation are high-energy consumption (reaction temperature >600 °C), partial conversion, catalyst coking and a selectivity around 90%. There have been various attempts to improve the process, such as oxidative dehydrogenation or the use of CO_2 as promoting reaction medium [12,13].

Although positive effects on conversion and selectivity have been observed, thermodynamics are prohibitive for the use of CO_2 as oxidant. The action of CO_2 in this reaction therefore remains unclear. Oxidative dehydrogenation is attractive, since the reaction becomes exothermic and complete conversion should be possible. Due to the lack of suitable catalysts, which have to operate at lower reaction temperatures, the selectivity achieved so far, does not exceed 90%. Most promising are instationary reaction conditions with conventional catalysts, where conversions of 97% at styrene selectivities >95% have already been realized [14].

In the present study, novel amorphous porous TiO_2-based mixed oxides are presented as potential catalysts for

* Present address: Taiyuan University of Technology, PR China.
** To whom correspondence should be addressed.

the oxidative dehydrogenation of ethylbenzene. Close to nothing is known about the catalytic properties of mixed oxides based on TiO_2. The catalysts have been prepared by a modified sol–gel process based on the procedure reported for the preparation of large surface area microporous TiO_2 [6]. Sol–gel procedures have succesfully been used in our laboratory in the past to prepare well defined silica catalysts for heterogeneously catalyzed reactions, such as esterification and etherification [15], selective oxidation of toluene [16], oxidative dimerization of propane [17], selective oxidation with organic hydroperoxides [18] or H_2O_2 [19] and shape selective hydrocracking [20]. The acid-catalyzed copolycondensation (sol–gel process), initiated by linear chain growth, leads to amorphous, porous mixed oxides (AM) with a narrow pore size distribution and large surface areas [21]. This is of fundamental importance for the catalytic properties, since mass transport and reaction kinetics are controlled by the pore architecture and microstructure of the catalysts.

2. Experimental

2.1. Catalyst preparation

The amorphous porous mixed oxides AM-M_xTi (x ranged from 1 to 5 mol%) were prepared by an acid-catalyzed sol–gel process in analogy to the following procedure: AM-Cr_5Ti: 9.6 ml $Ti(OiPr)_4$ was dissolved in 20 ml ethanol and stirred in a 250 ml PP-beaker for 15 min, then 480 μl 12 N HCl was added and after another 5 min of stirring 40 μl 8 N HCl were added and stirred for 1 h. Then 0.49 g chromium(III)-chloride hexahydrate in 6.47 ml ethanol, which has been mixed and stirred for 30 min, were added. Then the beaker was covered with parafilm and stored overnight under stirring until the sol converted into a gel. The gel was dried and calcined under ambient air according to the following program:

$$20\,^{\circ}\mathrm{C} \xrightarrow{0.5\,^{\circ}\mathrm{C/min}} 65\,^{\circ}\mathrm{C}\ (180\ \mathrm{min}) \xrightarrow{0.5\,^{\circ}\mathrm{C/min}}$$
$$250\,^{\circ}\mathrm{C}\ (180\ \mathrm{min}) \xrightarrow{2\,^{\circ}\mathrm{C/min}} \text{room temperature.}$$

For the other active metal centers the same procedure was applied, but the following precursors in place of the above mentioned chromium(III)-chloride hexahydrate have been used: $MnCl_2$, Fe(III)$(acac)_3$, Fe(II)Cl_2, $CrCl_3{\cdot}(H_2O)_6$, OV(IV)$(acac)_2$, Ce$(OiPr)_4$, $SbCl_3$, WCl_4, $IrCl_4{\cdot}H_2O$, $Na_2PtCl_6{\cdot}6H_2O$, $CoCl_2{\cdot}6H_2O$, Cu(I)Cl, Cu(II)Cl_2, $NiCl_2{\cdot}6H_2O$, $RuCl_3$, $PdCl_2$, $ZnCl_2$.

2.2. Catalytic activity test

A glass tube reactor with ∅ 6 mm i.d., 400 mm length was selected, about 300 mg catalyst was used per run, the reaction lasted for 0.5 h. Figure 1 shows the flowchart of the reaction system for oxidative dehydrogenation of ethylbenzene (EB). The figure 1 shows the reactor in vertical operation, which was only used in the long-time performance test. In all other experiments the reactor was positioned hoizontally. For routine operation all catalysts were ground in an agate mortar and the particle size of them was below 20 μm. The reaction temperature was kept for a minimum of 5 min after the syringe needle was inserted into the tube, before the EB was added by a syringe pump to the feed gas synthetic air. If not mentioned otherwise, the feed gas (flow rate 50 ml/min) was composed of 85 vol% air and 15 vol% EB (O_2 : EB = 1.13). The reaction products were collected in a U-tube cooled with dry ice and then analyzed by GC. The CO_2 in the product gas was monitored by an IR gas sensor (Winter).

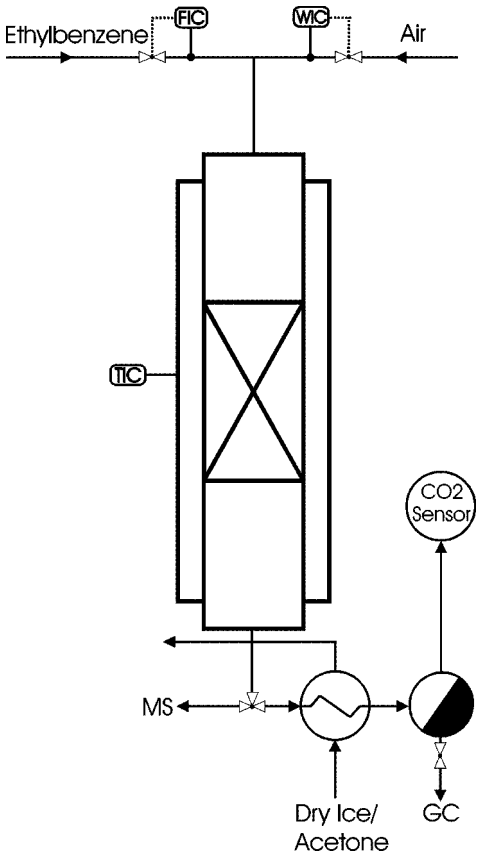

Figure 1. Flowchart of the reactor for the oxidative dehydrogenation of EB with synthetic air.

2.3. GC analysis

The samples from oxidative dehydrogenation of ethylbenzene were analyzed by gas chromatography using a GC-14A (SHIMADZU) with FID (detector at 220 °C) and a 30 m RTX-1 capillary column. Helium served as carrier gas.

2.4. On-line mass spectrometry

A Dycor M200 gas analyzer (quadrupole) was used to monitor products and analyse time dependency of product composition.

2.5. Catalyst characterization

2.5.1. Physisorption

The catalysts were outgassed prior to the measurement at 523.15 K and 10^{-4} mbar for 12 h. Using a modified Omnisorp 360 from Coulter (USA) adsorption isotherms were recorded in static volumetric technique with a starting pressure of 5 Torr, which was increased by a factor of 1.05 by each dosage step. Argon was used as analysis gas at 87.4 K. The system dead volume with the sample was measured with helium at analysis bath temperature. The ADP software, version 3.03 (Porotec) was used to calculate pore size distributions on the basis of the Horvath–Kawazoe model using a nitrogen on carbon potential at 77 K.

2.5.2. XRD measurement

X-ray powder diffraction was used to analyze the structure of the catalysts before and after reaction by a STOE powder diffractometer using curved germanium(III) as monochromator and Cu as target.

2.5.3. Light microscopy

An optical microscope (Optiphot-2, Nikon) with a RICOH camera (KR-10m) was used to examine the particle size of the catalysts.

2.5.4. HRTEM/EDX

The catalysts were examined with high-resolution transmission electron microscopy (HRTEM) on a HITACHI HF2000 instrument combined with energy dispersive X-ray analysis (EDX). The elemental distribution was investigated by selected area EDX microanalyses with area sizes varying from 2 nm to several micrometers. The samples were ground in an agate mortar in a methanol suspension and supported on a Cu-Holey-carbon grid (∅ 3 mm).

2.5.5. TGA

In order to analyze the catalyst's stability during reaction and the amount of "coking" on the catalyst after a long reaction time, thermogravimetric analysis (SHIMADZU TGA 150) was employed. Samples were heated at 10 °C/min to 650 °C in air.

2.5.6. Catalyst identification

Due to the high reaction temperature the catalysts used here have lost their narrow micropore size distribution. However, they remain amorphous and we therefore identify them as amorphous porous mixed oxides, AM-M_xTi, where x stands for the molar percentage of active metal oxide relative to the basic porous titanium oxide.

3. Results and discussion

3.1. Catalytic activity

Since very little is known about the behavior of dispersed active centers in the porous matrix of TiO_2, the dehydrogenation of ethylbenzene was studied over a broad temperature range (200–400 °C) with a variety of AM-M_xTi catalysts. Total combustion is the main side reaction, whose contribution increases with increasing temperature. Main liquid by-products are benzene and toluene; in some cases considerable amounts of benzaldehyde and benzofuran are obtained. The most promising results, summarized in table 1, have been obtained at 350 °C. The selectivities given do not include the gaseous products, since no quantitative gas analysis and no mass balance could be performed. The upper limit of the detection range of the CO_2-sensor used in initial experiments was 7%. Therefore values close to 7% may just represent a lower limit and should only be taken as a qualitative indication. The CO_2 data, taken from the readout of the on-line CO_2-sensor, are not corrected.

Remarkable activity and selectivity was observed for the Cu(I)-, Fe(II)-, Fe(III)-, V(IV)-, Ag-, Sb-, W-, Ru- and Cr-containing porous TiO_2 catalysts. However, even the undoped porous AM-Ti catalyst displays a remarkable actvity and selectivity, which renders some of the dopants (such as Ir or Ce) deactivating rather than activating. High activity, but low selectivity was observed for the Pt-, Pd- and Cu(II)-containing catalysts. The highest activity with associated high styrene selectivity at this relatively low temperature was obtained with the AM-Cr_5Ti. This catalyst was therefore selected to study the reaction behavior of these TiO_2-based catalysts in more detail. In all further experiments, a CO_2-sensor with a detection range of 0–20% could be used, so mass balances could be obtained.

To examine the influence of the Cr content in Cr_xTi on its activity, the Cr content was varied (1, 3 and 5%). No significant dependence of selectivity and conversions on the Cr content could be detected (see table 2).

All product compositions reported here have been obtained after 35 min at stationary conditions. The reactions were carried out at 15 vol% ethylbenzene in air to avoid the explosion range of 1–10 vol%. Because of the operation near the explosion limits no reaction order in ethylbenzene or oxygen has been obtained. Figure 2 shows the MS-trace of selected ions over time in a typical experiment with the AM-Cr_5Ti catalyst. At time zero the needle of the syringe pump is inserted into the air flow. The inital response is due to EB evaporation from the needle. After 5 min, when the evaporation has slowed down significantly, the syringe pump is started. Steady state behavior is reached already after 1 min. The data are uncorrected and do not correlate with absolute concentration, since ionization probabilities of the selected ions have not been corrected for and EB itself has an intensive fragment at $m/e = 78$. A rather constant styrene formation can be observed, although slow deactivation may occur. According to GC analysis, benzofuran, toluene and H_2O were also produced as by-products. GC data were obtained from integral product collection in the cold trap over all 30–35 min of reaction time. Sebbar [22] suggested the following sequential mechanism for the dehydrogenation of

Table 1
Results of oxidative dehydrogenation of ethylbenzene in synthetic air.[a]

AM-M_xTi catalyst	EB conversion (%)	Selectivity of products (%)					CO_2[b] (vol%)
		Benzene	Toluene	Styrene	Benzaldehyde	Benzofuran	
Without cat.	0.1	0.0	41.0	55.0	0.0	0.0	0.1
Ti	5.6	10.3	4.1	80.4	3.1	2.1	4.2
Mn_3Ti	1.2	0.0	2.5	92.9	4.5	0.0	0.1
Co_3(II)Ti	1.9	5.9	2.6	84.4	1.5	5.4	0.5
Cu_3(II)Ti	5.4	33.4	3.1	62.4	0.0	1.1	7.2
Cu_3(I)Ti	7.4	13.1	1.4	81.3	2.0	2.0	7.0
Fe_3(III)Ti	11.5	8.6	2.9	84.4	2.6	1.4	7.0
Fe_3(II)Ti	13.8	5.8	3.5	86.8	2.2	1.7	7.0
Ni_3Ti	8.6	8.2	2.8	85.5	0.6	2.8	7.4
V_3(IV)Ti	19.4	6.9	1.8	81.6	8.8	0.9	7.5
Cr_1Ti	18.7	24.8	2.5	70.9	2.2	0.6	6.6
Cr_3Ti	27.2	23.5	1.0	71.6	3.5	0.3	6.5
Cr_5Ti	28.6	21.4	0.8	75.5	2.1	0.2	7.3
Zn_3Ti	2.7	1.5	1.6	91.2	3.7	2.3	1.2
Ru_1Ti	3.9	12.2	8.4	79.4	0.0	0.0	6.0
Ru_3Ti	2.1	9.9	19.0	70.6	0.0	0.0	6.7
Pd_2Ti	8.9	33.2	18.1	48.6	0.0	0.0	7.3
Ag_2Ti	11.5	19.4	0.9	78.8	0.4	0.5	7.1
Ir_1Ti	1.6	6.8	4.2	89.6	0.0	0.0	7.4
Ir_3Ti	2.3	22.1	11.1	66.8	0.0	0.0	7.1
Pt_1Ti	1.5	28.0	29.3	42.7	0.0	0.0	7.4
Pt_2Ti	7.3	26.5	41.2	32.3	0.0	0.0	7.4
Ce_3(IV)Ti	1.0	0.0	5.0	88.8	6.2	0.0	0.6
Sb_3Ti	5.2	13.9	0.9	81.6	1.8	1.8	5.7
W_3Ti	17.9	15.2	1.2	75.2	7.1	1.3	6.5

[a] Reaction conditions: $T = 350\,^{\circ}C$, $P = 1$ atm, $W_{cat} = 300$ mg, flowrate of air = 50 ml/min, 15 vol% ethylbenzene.
[b] Data are uncorrected readouts from the CO_2 sensor.

Table 2
Results of oxidative dehydrogenation of ethylbenzene using Cr_xTi catalysts under different reaction temperatures.

Catalyst	RT (°C)	EB conversion (%)	Selectivity of products (%) excluding CO_2					CO_2 (vol%)
			Benzene	Toluene	Styrene	Benzaldehyde	Benzofuran	
Cr_1Ti	350	18.66	24.76	2.52	70.85	2.20	0.64	6.57
Cr_3Ti	350	27.19	23.54	1.03	71.57	3.53	0.27	6.51
Cr_5Ti	350	28.55	21.40	0.81	75.45	2.14	0.18	7.33

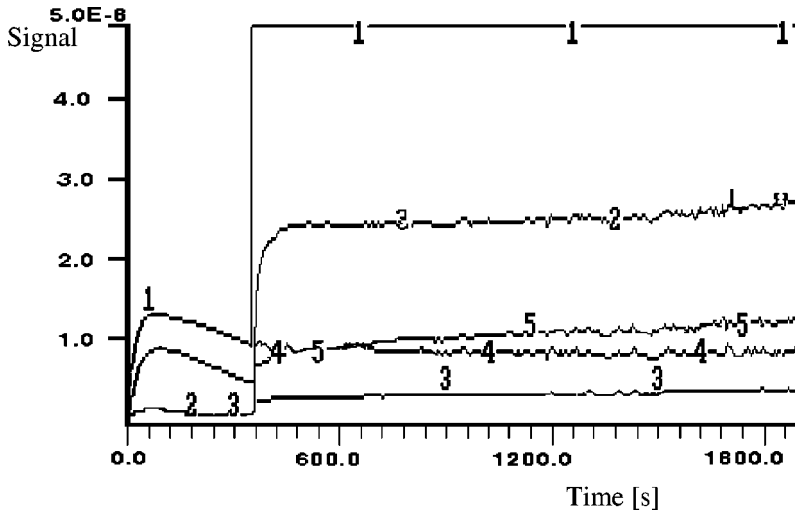

Figure 2. Time-dependent MS analysis of product composition of EB dehydrogenation over the AM-Cr_5Ti catalyst at 350 °C. Uncorrected molecular ions intensities (m^+ given in parentheses) were used to follow the product composition with time. 1 – CO_2 (44), 2 – benzene (78), 3 – toluene (92), 4 – styrene (104) and 5 – ethylbenzene (106).

ethylbenzene:

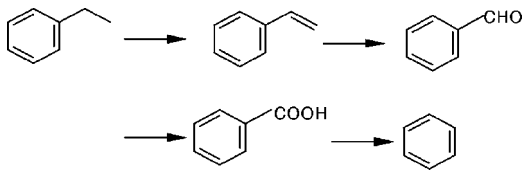

Our experiments can be explained by this mechanism, except that benzoic acid could not be detected, most likely due to a too low steady state concentration.

3.2. Effect of particle size on the activity of AM-Cr_5Ti

The effect of particle size on the catalytic activity of AM-Cr_5Ti was investigated. Six different particle sizes (20–500 μm) were obtained from a freshly prepared catalyst by grinding in a mortar, milling in a ball mill and sieving. A common problem in such a procedure is the contamination of the larger particle fragments by smaller particles, which tend to adhere to the surface of the larger particles by electrostatic effects. Special care was taken to avoid this and all sieve fractions have been controlled by light microscopy. The effect of catalyst particle size on conversion is shown in figure 3. All data were obtained after 35 min on stream. With decreasing particle size the activity of AM-Cr_5Ti increases, indicative of pore diffusion limitations. The highest activity was obtained with the particle size fraction of 20–50 μm or smaller.

The particle size 20–50 μm was selected to study the long-time performance of the catalyst under standard reaction conditions at 350 °C. Due to continuing problems with bed spreading in horizontal operation the reactor was operated vertically. Figure 4 shows the long-time performance of the AM-Cr_5Ti catalyst.

The catalyst exposed a remarkably constant activity over a very long reaction time. There was no sign of coking or other deactivation effect. For comparison the fresh and used AM-Cr_5Ti catalysts have been characterized by a variety of methods. X-ray powder diffraction confirmed, that the catalyst remains completely amorphous. There is no indication of crystallinity in both diffractograms confirming an unexpected stability of the amorphous nature of this mixed oxide. In figure 5 HRTEM micrographs of the fresh and the used catalysts are shown. The micrographs confirm the amorphous nature of the two catalysts, although some crystallization to nanometer-sized crystallites can be identified.

Selected area EDX on the catalyst documents a homogeneous elemental distribution. No indication of Cr-rich domain formation in the fresh and used catalyst and a constant Cr/Ti ratio are further evidence for stability of the chemical composition during catalysis. This is rather remarkable, since pure sol–gel derived amorphous TiO_2 tends to crystallize easily at temperatures above 300 °C. Similar results have been reported by Kumar and by Slunecko [23,24]. Slunecko proposed that the surrounding humidity during gelation is the key factor which decides the structure of gel. A significant influence of the relative humidity during the calcination on the crystallinity was observed.

Despite this morphological stability, there is a slight loss of total surface area in the used catalyst. After reaction the specific surface area of AM-Cr_5Ti decreased from 51 to 40 m^2/g. Figure 6 shows the pore size distribution of the catalysts and as an insert the isotherms of the catalysts.

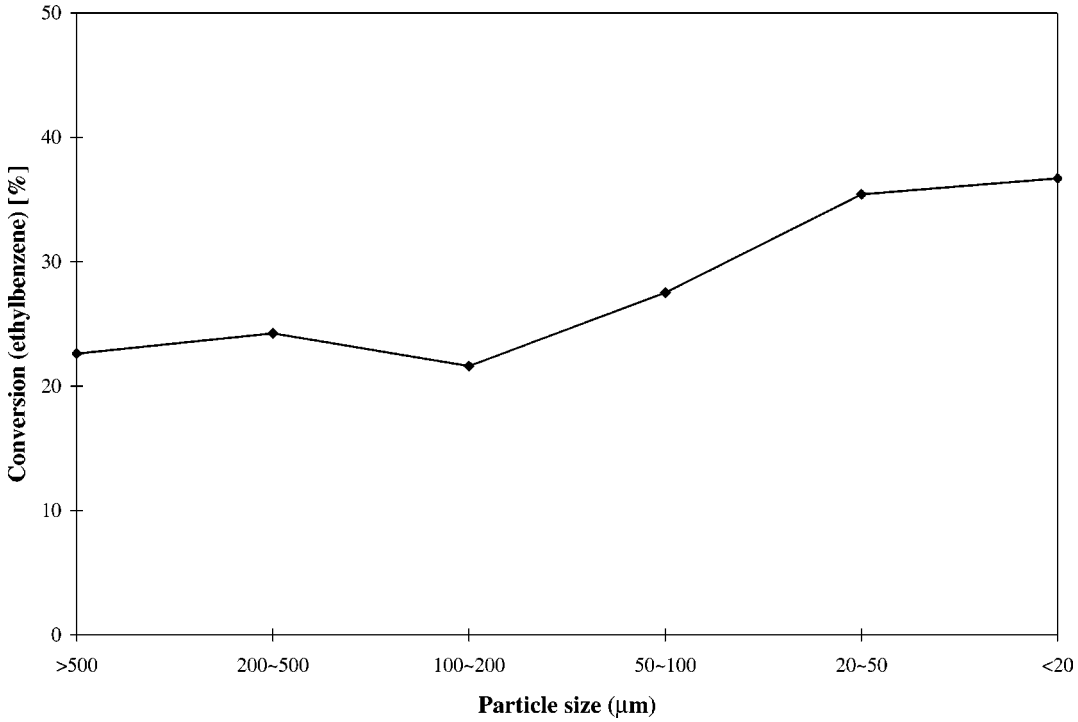

Figure 3. Effect of particle size on the catalytic activity of Cr_5Ti mixed oxides at 350 °C.

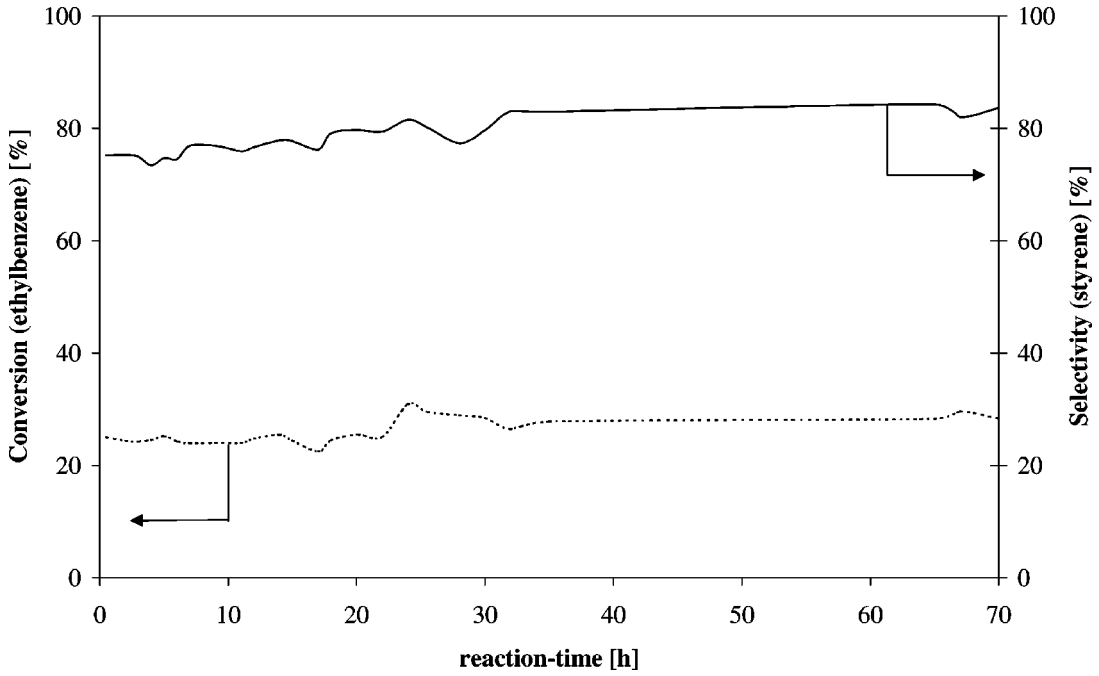

Figure 4. Long-term activity of Cr_5Ti mixed oxides at 350 °C.

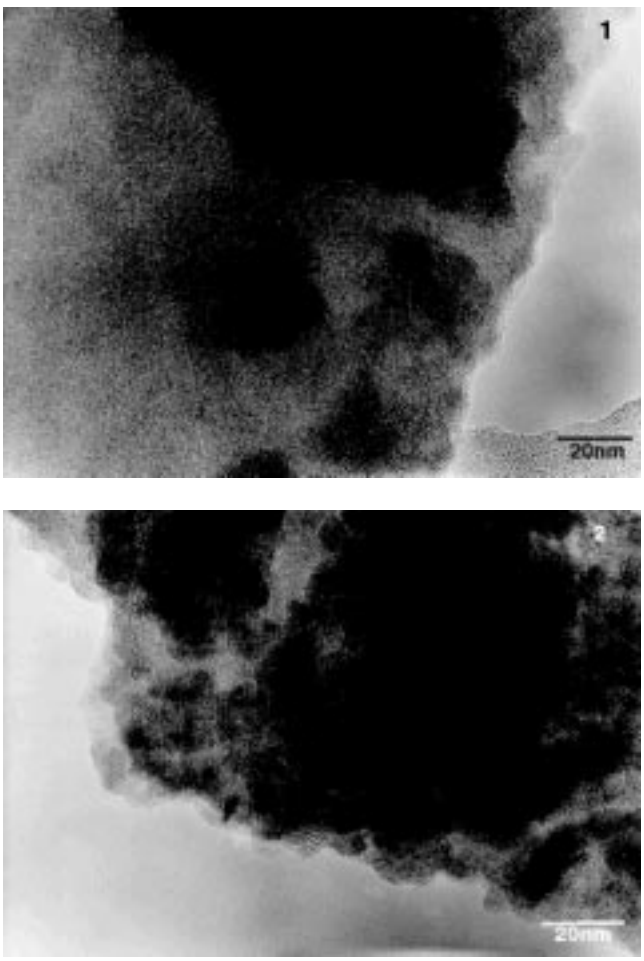

Figure 5. HRTEM/EDX comparable analyses of Cr_5Ti mixed oxides catalyst before and after reaction: (1) fresh and (2) used.

Table 3
HRTEM/EDX results of Cr_5Ti mixed oxides before and after reaction (wt%).

	Cr[a]	Ti[a]	C	Al[b]	Si[b]	Cu[c]
Fresh	5.82(4.11)	76.21(47.29)	–	–	–	15.20
Used	5.42(3.60)	59.74(51.99)	(3.35)	4.65	14.55	15.93

[a] The data in parentheses are from ICP.
[b] These elements are from glass wool as filling during reaction.
[c] Copper data are from the sample holder for TEM/EDX analyzing.

The materials are mesoporous with no indication of microporosity (no point of inversion at low p/p_0 in the high-resolution isotherms [25]). Here should be mentioned, that the freshly prepared catalyst, when calcined at 250 °C, has a total surface area of 106 m^2/g, but after calcination at 400 °C the surface area drops to 51 m^2/g. There is a significant reduction of the smaller pores in the fresh catalyst resulting in a shift of the pore size distribution from a maximum in the mesopore size distribution of about 3.5 to 5 nm in the used material. This change in microstructure apparently does not affect the catalytic performance.

Surface coking as potential source for catalyst degrading was investigated by TGA, elemental analysis, and EDX.

In table 3 elemental analysis (ICP) shows a total carbon content of 3.35% on the used catalyst, while no carbon was found on the fresh material (EDX cannot be used for C analysis due to the C content of the grids used). The chemical composition of the catalysts remained reasonably constant, as shown by EDX and ICP. The TGA data, obtained in air, are indicative of the loss of surface water of the fresh catalysts at temperatures around 100 °C, while both catalysts show a relatively sharp weight loss above 400 °C attributed to oxidation of surface carbon.

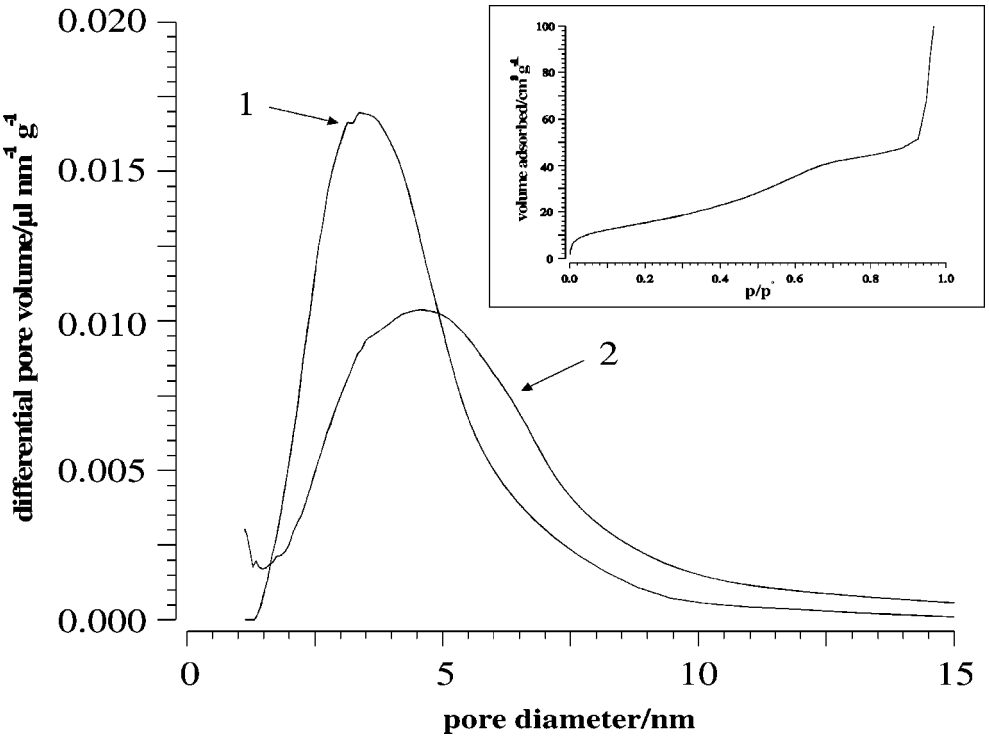

Figure 6. Physisorption results of Cr_5Ti mixed oxides catalyst: (1) fresh and (2) used.

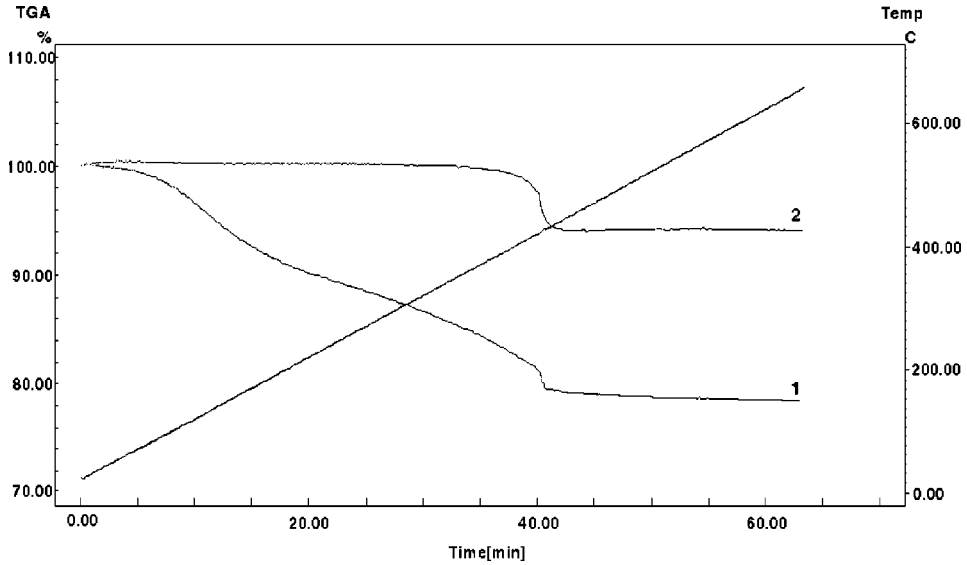

Figure 7. TGA results of Cr_5Ti mixed oxides catalyst before and after reaction: (1) fresh and (2) used.

These data indicate, that there is no substantial catalyst coking or leaching during the reaction. The significant changes in pore size and loss of surface area with time do not affect the catalytic performance.

4. Conclusions

Highly porous transition-metal-doped amorphous titanium oxides, prepared by an acid-catalyzed sol–gel procedure, are promising new catalysts for the oxidative dehydrogenation of ethylbenzene. The reaction proceeds at the attractive low temperature of 350 °C. These catalysts, which already reach 75% styrene selectivity at almost 30% conversion, may offer an alternative to today's high-temperature processing conditions.

Acknowledgement

WYL thanks the National Education Committee in China for support. We thank H. Bretinger for the determination of adsorption isotherms and S. Palm for powder X-ray diffraction.

References

[1] Y. Liu, Y.D. Zhang, X.X. Liu, J.Z. Xue and S.B. Li, Chem. Lett. 10 (1998) 1057.
[2] R. Grabowski, B. Grzybowska, A. Kozlowska, J. Sloczynski, K. Wcislo and Y. Barbaux, Catal. Lett. 3 (1996) 277.
[3] Y.M. Liu, Y. Lu, P. Liu, R.X. Gao and Y.Q. Yin, Appl. Catal. A 170 (1998) 207.
[4] J. Miki, Y. Osada, T. Konoshi, Y. Tachibana and T. Shikada, Appl. Catal. A 137 (1996) 93.
[5] E. Sanchez, T. Lopez, R. Gomez, Bokhimi, A. Morales and O. Novaro, J. Solid State Chem. 122 (1996) 309.
[6] W.F. Maier, I.-C. Tilgner, M. Wiedorn and H.-C. Ko, Adv. Mater. 5 (1993) 726.
[7] C.G. Guizard, A.C. Julbe and A. Ayral, J. Mater. Chem. 9 (1999) 55.
[8] H. Kisch, L. Zang, C. Lange, W.F. Maier, C. Antonius and D. Meissner, Angew. Chem. 110 (1998) 3201; Int. Ed. 37 (1998) 3034.
[9] *Ullmann (5)*, Vol. A25 (1994) p. 329.
[10] R.A. Sheldon and J. Dakka, Catal. Today 19 (1994) 215.
[11] J.A. Moulijn, P.W.N.M. van Leeuwen and R.A. van Santen, Stud. Surf. Sci. Catal. 79 (1993) 43.
[12] T. Badstube, H. Papp, P. Kustrowski and R. Dziembaj, Catal. Lett. 55 (1998) 169.
[13] J.S. Chang, J. Noh, S.E. Park, W.Y. Kim and Ch.W. Lee, Bull. Korean Chem. Soc. 19 (1998) 1342.
[14] O. Watzenberger, E. Ströfer and A. Anderlohr, Chem. Eng. Technol. 71 (1999) 150.
[15] S. Storck, W.F. Maier, S.I.M. Miranda, J.M.F. Ferreira, D. Guhl, W. Souverijns and J.A. Martens, J. Catal. 172 (1997) 414.
[16] F. Konietzni, U. Kolb, U. Dingerdissen and W.F. Maier, J. Catal. 76 (1998) 527.
[17] S. Bukeikhanova, H. Orzesek, U. Kolb, K. Kühlein and W.F. Maier, Catal. Lett. 50 (1998) 93.
[18] S. Klein, S. Thorimbert and W.F. Maier, J. Catal. 163 (1996) 477.
[19] S. Klein and W.F. Maier, Angew. Chem. 108 (1996) 2376; Int. Ed. 35 (1996) 2330.
[20] W.F. Maier, S. Klein, J. Martens, J. Heilmann, R. Parton, K. Vercruysse and P.A. Jacobs, Angew. Chem. 108 (1996) 222; Int. Ed. 35 (1996) 180.
[21] I.-C. Tilgner, P. Fischer, F.M. Bohnen, H. Rehage and W.F. Maier, Micropor. Mater. 5 (1995) 77.
[22] N. Sebbar, M. Haid and K. Griesbaum, in: *30th Tech. Phys. Chem. Conf.*, Karlsruhe, 1995, CA section 25, 100.
[23] K.N.P. Kumar, K. Keizer and A.J. Burggraaf, J. Mater. Sci. Lett. 13 (1994) 59.
[24] J. Slunecko, M. Kosec, J. Holc, G. Drazic and B. Orel, J. Am. Ceram. Soc. 81 (1998) 1121.
[25] S. Storck, H. Bretinger and W.F. Maier, Appl. Catal. A 174 (1998) 137.